# Potential sites for Asparagopsis spp. cultivation on Australia's East Coast in 2100

**Gabrielle King**

gkin2695@uni.sydney.edu.au

The University of Sydney

**Tristan Salles**

The University of Sydney

**Ana Vila-Concejo**

The University of Sydney

**Research Article**

**Keywords:** Species distribution models (SDM), Asparagopsis, Net Zero, Cultivation, Methane, Livestock

**Posted Date:** October 31st, 2025

**DOI:** https://doi.org/10.21203/rs.3.rs-7784217/v1



**Additional Declarations:** No competing interests reported.

# Abstract

*Asparagopsis*, a red macroalgae native to Australia's East Coast (10° S, 142° E to 44 ° S, 154° E), has shown the potential to reduce livestock methane emissions by up to 98%, facilitating climate change mitigation. Ensemble species distribution models were used to predict suitable cultivation sites for *A. armata* and *A. taxiformis* along the East Coast of Australia in 2100 under three climate scenarios (SSP-1, SSP-2, SSP-5). Results show a substantial loss of highly suitable habitat by 2100, with only moderately suitable areas remaining; one location for *A. armata* under SSP1-2.6, and four locations across multiple climate scenarios for *A. taxiformis*. Cultivating *Asparagopsis* in these locations can contribute to global methane mitigation efforts.


# 1 INTRODUCTION

Livestock production is the largest contributor to anthropogenic methane emissions (Camer-Pesci et al. 2023). Additionally, methane has a 28 times greater global warming potential than carbon dioxide over a 100-year period (Myhre et al. 2014). Further, demand for livestock derived products such as meat and milk is projected to increase by almost 40% by 2050 relative to 2020 levels (Komarek et al. 2021), accentuating the need to lower emissions from the livestock sector. More than 140 countries have committed to limiting global warming to a maximum of 2°C by 2100 under the Paris Agreement (UNFCCC n.d.), and major emitters, such as the United States of America and China, as well as Australia (the 14th greatest emitter), have set targets of Net Zero by 2050 (Friedrich et al. 2023; Department of Climate Change n.d.).

One promising methane mitigation strategy involves the use of the two species of the red macroalgae *Asparagopsis, A. armata* and *A. taxiformis*, as a livestock feed additive. Supplementing ruminants' diets with as little as 0.2% of this macroalga can reduce methane emissions by up to 98% (Kinley et al. 2020). Considering its potential, Australia's national science agency the CSIRO established the FutureFeed initiative in 2020 to commercialise *Asparagopsis* as a feed additive. FutureFeed currently holds the global intellectual property rights for its application and has identified the need to significantly scale up production to meet global demand and reduce costs. Yet, climate change adds complexity, as it is expected to alter macroalgal physiology and geographic distribution (Assis et al. 2016; Laeseke et al. 2020; Gonzalez-Aragon et al. 2024). Currently, only two of the nine licensed *Asparagopsis* farms worldwide are ocean-based, despite the greater costs associated with land-based cultivation (GreenerGrazing n.d.), underscoring the importance of identifying additional ocean-based cultivation sites under future climate conditions.

Five of FutureFeed's licensed farms are located in Australia, including one on the East Coast which lies within the native range of both *A. armata* and *A. taxiformis* (Zanolla et al. 2022; FutureFeed 2024). Both species do not generally occur simultaneously due to thermal tolerance differences. *A. armata* is principally found in cooler waters in the south and *A. taxiformis* in warmer waters in the north (Zanolla et al., 2022), thereby increasing the spatial extent of potentially suitable sites for cultivation by 2100. Yet,

this region is undergoing rapid oceanographic changes due to the intensification of the East Australian Current (EAC), which is projected to strengthen and extend southward while weaken in the north (Ridgway and Hill 2009; Oliver and Holbrook 2014; Bull et al. 2020). As a result of this, sea surface temperatures (SST) along Australia's East Coast are expected to increase by 2.5°C by 2050 and by up to 3.0°C by 2070 (Hobday and Lough 2011), with implications for the future distribution and viability of *Asparagopsis* cultivation.

This study aims to assess the impact of climate change on the distribution of *Asparagopsis spp.* along Australia's East Coast under three Shared Socioeconomic Pathways (SSPs): SSP-1(2.6) (low carbon emissions), SSP-2 (medium carbon emissions), and SSP-5 (high carbon emissions). Using species distribution models (SDMs) that correlate known species occurrences with environmental factors (Chaabani et al. 2019; Blanco et al. 2021; O'Mahony et al. 2021), the current (2010) and projected (2100) distributions of *A. armata* and *A. taxiformis* were modelled. The results identify locations that may remain suitable for cultivation in 2100, helping guide future investment in ocean-based *Asparagopsis* farming, and supporting methane mitigation efforts in the livestock sector.

## 2 MATERIAL & METHODS

Our study area extends over Australia's East Coast, ranging from 10° S, 142° E to 44 ° S, 154° E (Fig. 1). This region was chosen as it lies within the native distribution of both *A. armata* and *A. taxiformis.*

# 2.1 Species Occurrence Data

# 2.1.1 Data sources

Occurrence records for both species were obtained from the Global Biodiversity Information Facility (GBIF) (gbif.org) as well as from the Atlas of Living Australia (ALA) (ala.org). Both are open-access biodiversity databases that collate and store species presence data from multiple sources. Both databases were used to maximise spatial coverage and to capture any differences in occurrence records across repositories.

# 2.1.2 Processing

To ensure ecological relevance, occurrence points located on land, often originating from herbarium or museum collections, were removed. Likewise, occurrence points located below the depth range of both species (25 m for *A. armata* and 30 m for *A. taxiformis* (Zanolla et al. 2022)) were excluded to reduce outliers. Duplicate records were removed to prevent oversampling of specific sites. To address spatial autocorrelation and reduce sampling bias, the study area was rasterised at a 1km resolution using bathymetric data, and limiting only one presence point was retained per grid cell (Varela et al. 2014; Castellanos et al. 2019). Overall, this resulted in 60 points for *A. armata* and 33 records for *A. taxiformis* (Fig. 1).

# 2.2 Environmental Data

## 2.2.1 Sources and Datasets

Environmental predictor variables were obtained from Bio-Oracle v3.0, a global marine dataset tailored for species distribution modelling (Tyberghein et al. 2012; Assis et al. 2024). A summary of the selected environmental variables, their temporal resolution, units, and ecological justification is provided in Table 1. Long-term minimum and maximum layers which represent the “long-term average of the yearly maxima and minima of a given decade” (Assis et al. 2024) were chosen as the aim of the study was to determine the long-term impact of climate change on the species distribution by 2100. Only surface layers were used, as both species are typically found at depths shallower than 30 m (Zanolla et al. 2022). The variable “depth” itself was excluded from the modelling process, as *Asparagopsis* is cultivated on suspended ropes of fixed lengths, rendering bathymetric depth less relevant to cultivation feasibility.

Table 1
Environmental factors and associated aggregations, units and timestep used as well as justification for inclusion in the model

| Factor (abbreviation) | Aggregation/s | Unit | Present Timestep | Justification |
|---|---|---|---|---|
| *Ocean temperature* *(thetao)* | ltmax, ltmin | °C | 2010–2019 | One of most determining factors of growth and reproduction of *Asparagopsis* (Zhu et al. 2021; Mihaila et al. 2024) |
| *Nitrate* *(no3)* | ltmax, ltmin | mmol $m^{-3}$ | 2010–2018 | Most growth limiting nutrient for seaweed (Roleda and Hurd 2019) |
| *Phosphate* *(po4)* | ltmax, ltmin | mmol $m^{-3}$ | 2010–2018 | Second most growth limiting nutrient for seaweeds (Roleda and Hurd 2019) |
| *Dissolved iron* *(dfe)* | ltmax, ltmin | mmol $m^{-3}$ | 2010–2018 | Essential nutrient in algae; affects electron transport chains in photosynthesis and respiration (Rijkenberg et al. 2014; Schoffman et al. 2016). |
| *Seawater speed* *(sws)* | ltmax | m $s^{-1}$ | 2010–2019 | Positive relationship with growth in *Asparagopsis* (Mihaila et al. 2024) |
| *Salinity* *(so)* | ltmax, ltmin | psu | 2010–2019 | Affects osmosis and turgor pressure (Nejrup and Pedersen, 2012; Pereira et al., 2017). |
| *pH* *(ph)* | ltmin | pH | 2010–2018 | Affects photosynthetic rates (Wootton et al. 2008; Britton et al. 2016). |

## 2.2.2 Processing

All environmental layers were cropped to the defined study area and limited to ocean regions shallower than 200 m to focus on coastal and shelf habitats. The layers were then interpolated to a spatial resolution of 1 km and extrapolated landward to extend to the coastline, ensuring continuous coverage across nearshore environments. Collinearity between environmental variables was not explicitly assessed, as several algorithms used within the ensemble SDM framework inherently account for multicollinearity. These include Random Forest (Boulesteix et al. 2012), eXtreme Gradient Boosting Training (Montomoli et al. 2021), and Maximum Entropy (Feng et al. 2019). In the context of predictive modelling rather than interpretive analysis, Multiple Adaptive Regression Splines (MARS) is also considered robust to collinearity (Li et al. 2020). In addition, studies have found that collinearity has less substantial effects on species extent when modelled by ensemble models rather than simple models (De Marco and Nóbrega 2018). For baseline modelling, environmental data from 2010–2018 (or 2010–2019, depending on availability see Table 1) were used to approximate current species distributions. Future projections for 2100 (Table 2) were based on three Shared Socioeconomic Pathways (SSPs) from the CMIP6: SSP-1(2.6), SSP-2, and SSP-5.

Table 2
Chosen SSP scenarios with associated predicted warming and emission trends

| SSP | Warming | Emissions track |
|---|---|---|
| *1(2.6)* | 2°C | Low radiative forcing. Emission reductions in near future |
| *2* | 3°C | Intermediate radiative forcing. Emissions increasing until 2040 and then decrease |
| *5* | 4°C | Increasing emissions until 2080 |

# 2.3 Modelling

Species distribution models were constructed using the biomod2 R package, an ensemble modelling platform that integrates multiple statistical and machine learning techniques (Thuiller et al. 2016). One ensemble model was developed for each species (*A. armata* and *A. taxiformis*) across the East Coast of Australia using 11 commonly applied SDM algorithms; Artificial Neural Network (ANN), Classification Tree Analysis (CTA), Generalized Additive Model (GAM), Maximum Entropy (MAXENT), Generalized Boosting Model (GBM), Multiple Adaptive Regression Splines (MARS), Flexible Discriminant Analysis (FDA), Random Forest (RF), Surface Range Envelop (SRE), eXtreme Gradient Boosting Training (XGBOOST), Maximum Entropy (MAXNET).

# 2.3.1 Pseudo absences

As no true absence data was available, 10,000 pseudo-absence points were randomly drawn from the study area and within the same depth range as each species. From these, a random subset of 1,000 pseudo-absences was chosen for model training for each species.

# 2.3.2 Model training and cross-validation

Each of the 11 modelling algorithms was trained using a repeated, random sub-sampling validation approach. Models were cross-validated by randomly partitioning the presence and pseudo-absence data into training and testing sets over ten iterations, as recommended in the biomod2 documentation (Thuiller et al. 2016). This procedure was repeated three times, each time using one-third of the pseudo-absence dataset. In total, 533 individual models were generated for each species.

### 2.3.3 Ensemble modelling and performance assessment

The projections derived from the individual models were then coalesced into an ensemble model by averaging the predictions across all qualified models (O'Mahony et al. 2021). This ensemble approach improves prediction accuracy and robustness, offering more realistic estimates of potential species distribution (Thuiller et al. 2009; Chaabani et al. 2019). The performances of the single and ensemble models were assessed by comparing for each algorithm, the Receiver Operating Characteristic curve (ROC), mean True Skill Statistic (TSS) and Cohen's Kappa Coefficient (Kappa). The main index used for evaluating the models' performance was TSS, which accounts for both sensitivity and specificity. Only models with a TSS score above 0.6 were included to build the ensemble model (Thuiller et al. 2009). The performances of the ensemble models were evaluated using the same criteria. The TSS metric was selected over commonly used alternatives such as ROC and Kappa, due to known limitations: ROC measures a model's ability to discriminate between presence and absence locations across all possible thresholds, but it is sensitive to the spatial extent of the modelling domain (Lobo et al. 2008; Beck et al. 2014). Kappa compares the observed accuracy of the model to what would be expected by chance, but it is highly sensitive to species prevalence, particularly when the number of occurrence points available is small. In contrast, TSS is not sensitive to extent or prevalence (Allouche et al. 2006).

## 2.4 Current and future predictions

Using the 2010 distribution predictions for each species, projections for their distribution under SSP-1 (2.6), SSP-2 and SSP-5 in 2100, were run.

Habitat suitability scores produced by the ensemble models ranged from 0 to 1000 and were then categorized into four categories using equal interval classification;

1. 0–250 as unsuitable,
2. 250–500 as poorly suitable
3. 500–750 as moderately suitable, and
4. 750–1000 as highly suitable.

Since each grid cell represents 1 $km^2$, the total area per suitability class corresponds directly to the number of pixels in that class.

# 3 RESULTS

## 3.1 Model performance

The ensemble models were evaluated using three aggregation approaches: the median, mean, and weighted mean of probabilities (wmean). For both *A. armata* and *A. taxiformis*, all three ensemble approaches achieved excellent performance with TSS scores above 0.95, ROC scores above 0.79, Kappa scores above 0.98 (Fig. 2), indicating excellent agreement between predicted and observed occurrences. Among the aggregation methods, the mean probability approach yielded the best overall performance across metrics. As such, subsequent figures and analyses are based on mean ensemble predictions (Fig. 2).

## 3.2 Environmental drivers of *Asparagopsis spp.* distributions

The optimal conditions of the five most important environmental factors affecting the distribution of both species can be seen in Table 3. As can be seen from Table 3 and Fig. 3, A. *armata* and *A. taxiformis* were influenced by distinct environmental variables, reflecting their contrasting thermal niches and habitat preferences (Zanolla et al. 2022). For both species, long-term dissolved iron and long-term maximum sea temperature are within the five most important environmental factors (Table 3; Fig. 3). The thermal differences between the two species can be seen from the optimal long-term maximum sea temperature (Table 3).

Table 3
Optimum conditions and standard deviation (SD) for five most important environmental factors (in descending order) affecting the distribution of *A. armata* and *A. taxiformis* respectively

| ***A. armata*** | | | |
|---|---|---|---|
| *Environmental factor* | *Unit* | *Optimum* | *± SD* |
| long-term minimum pH | pH | 8.053 | 0.016 |
| long-term maximum dissolved iron | mmol $m^{-3}$ | 0.003 | 0.001 |
| long-term maximum sea temperature | ° C | 20.508 | 2.033 |
| long-term minimum phosphate | mmol $m^{-3}$ | 0.119 | 0.051 |
| long-term minimum nitrate | mmol $m^{-3}$ | 0.167 | 0.403 |
| **A. taxiformis** | | | |
| *Environmental factor* | *Unit* | *Optimum* | *± SD* |
| long-term maximum dissolved iron | mmol $m^{-3}$ | 0.004 | 0.001 |
| long-term maximum sea temperature | ° C | 28.661 | 1.092 |
| long-term minimum sea temperature | ° C | 21.449 | 1.493 |
| long-term minimum salinity | psu | 34.682 | 0.550 |
| long-term maximum salinity | psu | 35.715 | 0.142 |

# 3.3 Suitable habitat for *Asparagopsis spp.* in 2010

The areas with suitable habitat for *Asparagopsis spp.* have been named with the label ROI (Region Of Interest) with an A (for *A. armata*) or T (for *A. taxiformis*) and numbered chronologically from north to south (Table 4; Fig. 4).

Table 4
Regions Of Interest (ROI) of A. armata (A) and A. taxiformis (T) and associated toponym and approximate coordinates

| | Label | Toponym | Coordinates |
|---|---|---|---|
| *A. armata* | ROIA1 | NSW coast | between 32 and 38°S, 150°40’ E |
| | ROIA2 | Melbourne | 38°08’S, 144°50’E |
| | ROIA3 | Tasmania east coast | between 40 and 43°S, 148°06’ E |
| *A. taxiformis* | ROIT1 | Lizard Island | 14°45’ S, 145°25’ E |
| | ROIT2 | Townsville | 18°46’ S, 146°23’ E |
| | ROIT3 | Gladstone | 23°37’ S, 151°18’ E |
| | ROIT4 | Brisbane | 27°20’ S, 153°17’ E |

Overall, in 2010, *A. armata* exhibited the greatest habitat suitability in the southern half of the study area (Fig. 4a). Highly suitable habitat (scores between 750–1000) accounted for 0.30% of the study area, equivalent to 12,240 $km^2$, and was concentrated in ROIA1, ROIA2 and ROIA3. Surrounding these zones were moderately suitable areas (scores between 500–750) which made up an additional 0.56% of the study area.

In contrast, *A. taxiformis* showed greatest suitability in the northern half of the study area, consistent with its higher thermal tolerance (Zanolla et al. 2022). Notable clusters of high suitability (750–1000) were identified at ROIT1, ROIT2, ROIT3, and ROIT4 (Fig. 4b; Table 4). This area covered 0.13% of the total study area, or 5,304 $km^2$. This is approximately 60% less than the area for *A. armata*. Areas of moderate (500–750) suitability accounted for an additional 0.36% and extended around the regions of high suitability.

# 3.3.1 Factors driving *A. armata* habitat suitability

Suitability in ROIA1 was driven by long-term minimum pH, phosphate and nitrate concentrations and long-term maximum sea temperatures which were optimal for *A. armata* according to the model. The suitability in ROIA2 and ROIA3 was driven by all five factors. Long-term minimum pH in the suitable areas of ROIA1, ROIA2 and in ROIA3 correspond to the optimal long-term minimum pH conditions of 8.053 ± 0.016 pH. In the three ROIs, long-term maximum dissolved iron concentrations are approximately 0.0015, 0.0025 and 0.002 mmol $m^{-3}$ respectively. The latter two (ROIA2 and ROIA3) correspond to the optimal concentrations for the growth of *A. armata* as determined by the model. Long-term maximum temperatures in the three ROIs all correspond to the optimal long-term maximum sea temperature conditions of 20.508 ± 2.033°C. Finally, in these regions, the long-term minimum concentrations of phosphate and nitrate are within the optimal conditions of 0.119 ± 0.051 mmol $m^{-3}$ and 0.167 ± 0.403 mmol $m^{-3}$ respectively.

### 3.3.2 Factors driving *A. taxiformis* habitat suitability

Suitability at ROIT1 was driven by long-term maximum and minimum sea temperature as well as long-term minimum and maximum salinity. Suitability at ROIT2 and ROIT3 was driven by all five factors. Suitability at ROIT4 was driven by long-term maximum sea temperature as well as long-term minimum and maximum salinity. Long-term maximum sea temperature at all four ROIs had the optimal conditions for the growth *of A. taxiformis* of 28.661 ± 1.092°C as determined by the model. The suitability in all ROIs were also all driven by long-term maximum salinity which had the optimal conditions of 35.715 ± 0.142 psu. The suitability in ROIT1, ROIT3 and ROIT4 was also driven by long-term minimum salinity with the optimal conditions of 34.682 ± 0.550 psu. The suitability in ROIT1, ROIT2 and ROIT3 was also driven by long-term minimum sea temperature with the optimal conditions of 21.449 ± 1.493°C. Long-term maximum dissolved iron at ROIT2 and ROIT3 was approximately 0.0038 and 0.003 mmol $m^{-3}$ respectively which corresponds to the optimal conditions of 0.004 ± 0.001 mmol $m^{-3}$.

## 3.4 Projected suitable Habitat for *Asparagopsis spp.* in 2100

By 2100, suitable habitat for both species of *Asparagopsis* is projected to decline substantially under all climate scenarios compared to 2010. Notably, no highly suitable habitat (750–1000) remains for either species under any of the SSP projections (Fig. 5; Fig. 6). For *A. armata*, only under SSP-1 (2.6) does some area of moderate (500–750) suitability persist in ROIA3, specifically at 49°55’ S, 147°22’ E (Fig. 5), comprising less than 0.01% of the total study area (Fig. 6). Under both SSP-2 and SSP-5, *A. armata* loses all moderately or highly suitable habitat.

Long-term maximum temperature in ROIA1 is 25°C under SSP-1 and increases to 26°C under SSP-2 and up to 28°C under SSP-5. This is above the optimal long-term maximum temperature determined by the model. Other factors have also made this area unsuitable; although the long-term minimum pH is suitable under SSP-1, it drops under the optimal pH of 8.053 ± 0.016 under SSP-2 and SSP-5. Further adding to the loss in suitability of the area is maximum dissolved iron concentration which in 2100 appears to be slightly lower than the optimal long-term maximum concentration of dissolved iron as predicted by the model of 0.003 ± 0.001 mmol $m^{-3}$.

For ROIA2 and ROIA3 the loss in suitability can be attributed in part to a rise in temperature; long-term maximum temperature in ROIA2 and ROIA3 ranges between 17–22°C under SSP-1, 18–23°C under SSP-2, and 20–25°C under SSP-5. These values under SSP-2 and SSP-5 in parts exceeds the optimal temperature of 20.508 ± 2.033°C as determined by the model. Therefore, the increasing temperature may be driving the loss of *A. armata* in this region as it starts to exceed the optimal conditions determined by the model. The reduction in suitability in these regions could also be attributed to changes in pH especially under SSP-2 and SSP-5 which show pH values below 8, lower than the optimal value.

*A. taxiformis* retains a slightly broader range of moderately suitable habitat (500–750) by 2100. Such areas account for 0.06% of the study area under SSP-1 (2.6), decreasing to 0.01% under both SSP-2 and SSP-5 (Fig. 6). Under SSP-1(2.6), small patches of moderate suitability for *A. taxiformis* remain near ROIT1, ROIT2, ROIT3, and ROIT4. Under SSP-2, only ROIT1 and ROIT2 maintain residual moderately suitable habitat. Under SSP-5, the area near ROIT1 maintains moderate suitability and a small area of moderate suitability reappears near ROIT4 (Fig. 5).

In ROIT1, the loss in suitability from high to moderate between 2010 and 2100 can first be attributed to the rise in temperature above the optimal long-term maximum temperature. A second reason can be that long-term maximum salinity is optimal in 2010 as well as under SSP-1, however, under SSP-2 and SSP-5, the salinity increases out of the optimal long-term maximum salinity range for *A. taxiformis.* In ROIT2 the loss in suitability between SSP-1 and SSP-2 can be attributed to the optimal long-term minimum and maximum temperatures being exceeded. The continued loss under SSP-5 can be attributed to long-term maximum salinity exceeding the optimal condition of 35.715 ± 0.142 psu. The complete loss between SSP-2 and SSP-5 of moderate suitability in ROIT3 can be attributed to long-term maximum temperature exceeding the optimal values as determined by the model. For ROIT4 it is difficult to determine a reason for the loss in suitability from high to moderate between 2010 and SSP-1 as well as loss from moderate to mainly poor between SSP-1 and SSP-2 in ROIT3, as between these scenarios there is not much fluctuation between the variables.

# 4 DISCUSSION

The aim of this study was to identify key locations most suitable for the growth of *Asparagopsis armata* and *taxiformis* on the East Coast of Australia in 2100 under three climate scenarios SSP-1(2.6), SSP-2 and SSP-5. These locations could then inform decisions cultivation sites of *Asparagopsis* in the future to help production demand for the livestock industry globally.

## 4.1 Potential cultivation sites in 2100 for *Asparagopsis spp.*

In 2100, no areas of high suitability exist in the study area for either species of *Asparagopsis*. Areas of moderate suitability exist for both species. Under SSP-1(2.6), there is less than 408 $km^2$ of moderately suitable area available in ROIA3 for *A. armata.* However, this is only a viable option if we follow the climate trajectories of SSP-1(2.6) as there are no moderately suitable areas left under the more intense climate scenarios. *A. taxiformis* has more suitable area than *A. armata*. Under SSP-1(2.6), 2,448 $km^2$ of moderately suitable area is available. Under the other climate scenarios more than 400 $km^2$ is available for *A. taxiformis*. The best locations for *A. taxiformis* cultivation would be near ROIT1 as it remains moderately suitable under all climate scenarios, ROIT2 remains moderately suitable under SSP-1(2.6) and SSP-2, ROIT3 that has moderate suitability under SSP-1(2.6), and ROIT4 remains moderately suitable under SSP-1(2.6) and SSP-5.

It should be considered that whilst areas of moderate suitability will be limited in 2100, not much area is necessary for productive cultivation of *Asparagopsis*. In 2004, eight tonnes of *A. armata* wet biomass was harvested from 14 km of cultivation rope in an area of 0.02 $km^2$ (Werner et al. 2004). According to FutureFeed (2024), to meet global demand, production of 100,000 tonnes per year will be needed. From this, assuming such values are based off bromoform concentrations as found in *A. armata*, a very rough estimate of area required to meet global demand results in a minimum of 250 $km^2$. As *A. taxiformis* has 8.5 times less bromoform than A. armata more than 2000 $km^2$ would be needed. Although the available areas are only moderately suitable in 2100, they are large enough to contribute significantly to the production of *Asparagopsis* globally. Other locations Australia-wide and globally may be available for *Asparagopsis* cultivation as currently *Asparagopsis* is cultivated in the ocean on Australia's west and south coast, in Vietnam and tests undergoing currently in south Korea indicating its widespread suitability.

# 4.2 Factors explaining the loss of suitable locations in 2100

Compared to 2010, in 2100 all highly suitable habitat is lost for both species under all climate scenarios. In terms of moderately suitable habitat, for *A. armata* more than 98% is lost under SSP-1(2.6) and 100% is lost under the more intense climate scenarios compared to 2010. For *A. taxiformis*, approximately 83% of moderate suitable habitat is lost under SSP-1(2.6) and more than 97% is lost under the more intense climate scenarios compared to 2010. This general loss in suitability can be attributed to unfavourable changes in environmental conditions. In 2010, areas were moderately or highly suitable if at least three of the five most important environmental factors affecting the distribution of the *Asparagopsis* species (Table 3) were in their optimal condition as determined by the model. If between 2010 and 2100 some of the environmental factors were no longer in their optimal conditions this resulted in a loss of suitability.

For both species, the loss of moderately and highly suitable area in 2100 can be particularly attributed to a rise in sea temperature. *A. armata* has an optimal long-term maximum temperature of 20.508 ± 2.033°C as determined by the model, and an upper thermal tolerance of either 21°C (Mihaila et al. 2024) or 24°C (Chualáin et al. 2004). Yet in 2100, in ROIA1, all these values are largely surpassed. In ROIA2 and ROIA3 under the different climate scenarios certain areas surpass the optimal temperature determined by the model but they never surpass the upper thermal tolerance as found by previous studies (Chualáin et al. 2004; Mihaila et al. 2024). Temperature may however not be driving the loss as sea temperature never completely exceeds the predicted optimal maximum temperature for *A. armata* or the upper thermal tolerances as found by previous studies (Chualáin et al. 2004; Mihaila et al. 2024). In addition, typically, seaweed growth increases with increasing temperature up to a certain limit which is the thermal tolerance of the species (Mihaila et al. 2024). *A. taxiformis*' optimal long-term maximum temperature is 28.661 ± 1.092°C and an upper thermal tolerance of 25–28°C (Zanolla et al. 2022). In 2100, both these values are surpassed for ROIT1, ROIT2 and ROIT3. This rise in temperature throughout the study region is probably a consequence of the lengthening and strengthening of the EAC bringing warmer water further south. In fact, the decline of giant kelp forests by more than 50% in 50 years in

Tasmanian (around ROIA2 and ROIA3) waters has been attributed to the lengthening of the EAC bringing warmer, nutrient poor waters towards the south of the east coast (Hobday et al. 2006; Ling 2008; Vergés et al. 2016). Globally, the loss of macroalgae due to rising temperatures has been well studied (Wilson et al. 2019). Temperature affects all aspects of macroalga growth as it regulates enzyme activity and diffusion of nutrients (Roleda and Hurd 2019; Theobald et al. 2024). Warmer water has a further detrimental impact on algae due generally to lower nutrient concentrations (Kämpf and Chapman 2016).

The general loss in suitability is not just due to rising sea temperature but also due to the compounding effect of multiple environmental factors no longer being in the optimal conditions. pH, the environmental factor which affected the distribution of *A. armata* the most according to the model, decreased in 2100 compared to 2010. According to Bio-Oracle, in 2100, under all climate scenarios, pH drops below the optimal long-term minimum pH of 8.053 ± 0.016 in all locations. Ocean acidification can limit the bio-availability of nutrients (Asadian et al. 2018). Nevertheless, multiple studies have found increases in non-calcifying macroalgae growth with reduced pH (Beardall et al. 1998; Cornwall et al. 2012). For *A. taxiformis*, the loss can also be partially attributed to salinity increases, surpassing the optimal long-term maximum salinity of 35.715 ± 0.142 psu in ROIT1 and ROIT2. Salinity is responsible for the distribution of algae globally and locally (Nejrup and Pedersen 2012; Pereira et al. 2017) as it plays a key role in osmosis and turgor pressure (Pereira et al. 2017). Pereira et al. (2017) showed that for a red macroalga, salinity level outside of 25–40 psu were very damaging, often resulting in reduced branching and thalli bleaching.

pH, salinity and iron are considered to be critical to the growth of algae. The importance of pH and salinity has been discussed previously. Iron is essential in plants, including algae, playing a vital role in electron transport chains in photosynthesis and respiration (Rijkenberg et al. 2014; Schoffman et al. 2016). The high importance in determining suitable habitat for *Asparagopsis spp.* that these factors were attributed by the model is surprising, given that other factors such as nitrate and phosphate have been shown to be extremely important variables affecting the growth of *Asparagopsis* (Roleda and Hurd 2019; Zhu et al. 2021). This could be a result of being inflated as these pH, salinity and iron do not fluctuate substantially within the study area and therefore between occurrence points (Harisena et al. 2021). This means that these environmental conditions represent more the conditions of the study area than the optimal growth conditions for the species.

# 4.3 Limitations and future research

This study has limitations sourced from the raw data and methodology which provides multiple opportunities for future research to build upon. Future studies will benefit from more precise data for the environmental factors. Further, the Bio-Oracle v3.0 environmental factors, derived from Earth System Models (ESMs) come with additional assumptions and limitations (Flato 2011; Heavens et al. 2013). *Asparagopsis* is clearly an adaptable genus, as attested by its invasive capabilities (Taylor and Kumar 2013; Blanco et al. 2021; Silva et al. 2021). Therefore, it is possible *Asparagopsis spp.* could undergo niche shifts under the future conditions (Laeseke et al. 2020). Future studies should integrate biological processes such as adaptation as they are fundamental to producing more accurate projections of the

distribution of a species (especially adaptable ones), such as by using ΔTraitSDMs (Benito Garzón et al. 2019).

Overall, this study demonstrated that the East Coast of Australia is a suitable area for the cultivation of *Asparagopsis spp.* under climate change in 2100. Under all climate scenarios, for *A. armata*, the southern region near ROIA3 will remain moderately suitable for cultivation under low emission scenarios (SSP-1(2.6)), and for *A. taxiformis* a few key sites, namely near ROIT1, ROIT2, ROIT3 and ROIT4, remain moderately suitable for cultivation under some or all climate scenarios in 2100. Increased production globally would render *Asparagopsis* products more accessible to the livestock industry, in turn assisting emissions reductions, facilitating countries to reach targets of NetZero.

# Declarations

Funding:No funds, grants, or other support was received.

Competing Interests:The authors have no competing interests to declare that are relevant to the content of this article.

Data availability

The data and notebooks will be made available via Zenodo [https://zenodo.org/].

### Authors' contributions

Gabrielle King, Tristan Salles and Ana Vila-Concejo contributed to the study conception and design. The first draft of the manuscript was written by Gabrielle King, Tristan Salles and Ana Vila-Concejo commented on previous versions of the manuscript. All authors read and approved the final manuscript.

# References

1. Asadian M, Fakheri BA, Mahdinezhad N, Gharanjik S, Beardal J, Talebi AF (2018) Algal communities: An answer to global climate change. CLEAN–Soil, Air, Water vol. 46, no. 10, pp. 1800032.
2. Assis J, Fernández Bejarano SJ, Salazar VW, Schepers L, Gouvêa L, Fragkopoulou E, Leclercq F, Vanhoorne B, Tyberghein L, Serrão EA (2024) Bio-ORACLE v3. 0. Pushing marine data layers to the CMIP6 Earth System Models of climate change research. Global Ecology and Biogeography vol. no., pp. e13813.
3. Assis J, Lucas AV, Bárbara I, Serrão EÁ (2016) Future climate change is predicted to shift long-term persistence zones in the cold-temperate kelp Laminaria hyperborea. Marine Environmental Research vol. 113, no., pp. 174-182.
4. Beardall J, Beer S, Raven JA (1998) Biodiversity of marine plants in an era of climate change: some predictions based on physiological performance. vol. 41, no. 1-6, pp. 113-123.

5. Benito Garzón M, Robson TM, Hampe A (2019) ΔTrait SDMs: species distribution models that account for local adaptation and phenotypic plasticity. New Phytologist vol. 222, no. 4, pp. 1757-1765.
6. Blanco A, Larrinaga AR, Neto J, Troncoso J, Méndez G, Domínguez-Lapido P, Ovejero A, Pereira L, Mouga T, Gaspar R (2021) Spotting intruders: Species distribution models for managing invasive intertidal macroalgae. Journal of Environmental Management vol. 281, no., pp. 111861.
7. Boulesteix AL, Janitza S, Kruppa J, König IR (2012) Overview of random forest methodology and practical guidance with emphasis on computational biology and bioinformatics. Wiley Interdisciplinary Reviews: Data Mining and Knowledge Discovery vol. 2, no. 6, pp. 493-507.
8. Britton D, Cornwall CE, Revill AT, Hurd CL, Johnson CR (2016) Ocean acidification reverses the positive effects of seawater pH fluctuations on growth and photosynthesis of the habitat-forming kelp, Ecklonia radiata. Scientific reports vol. 6, no. 1, pp. 26036.
9. Bull CY, Kiss AE, Gupta AS, Jourdain NC, Argüeso D, Di Luca A, Sérazin G (2020) Regional versus remote atmosphere-ocean drivers of the rapid projected intensification of the East Australian Current. Journal of Geophysical Research: Oceans vol. 125, no. 7, pp. e2019JC015889.
10. Camer-Pesci B, Laird DW, van Keulen M, Vadiveloo A, Chalmers M, Moheimani NR (2023) Opportunities of Asparagopsis sp. cultivation to reduce methanogenesis in ruminants: A critical review. Algal Research vol. 76, no., pp. 103308.
11. Castellanos AA, Huntley JW, Voelker G, Lawing AM (2019) Environmental filtering improves ecological niche models across multiple scales. Methods in Ecology and Evolution vol. 10, no. 4, pp. 481-492.
12. Chaabani S, López-González PJ, Casado-Amezú P, Pehlke H, Weber L, Martínez-Baraldés I, Jerosch K (2019) Ecological niche modelling of cold-water corals in the Southern Ocean (N Antarctic), present distribution and future projections due to temperature changes. Marine Ecology Progress Series vol. 628, no., pp. 73-93.
13. Chualáin FN, Maggs CA, Saunders GW, Guiry MD (2004) The invasive genus Asparagopsis (bonnemaisoniaceae, rhodophyta): molecular systematics, morphology, and ecophysiology of falkenbergia isolates 1. Journal of Phycology vol. 40, no. 6, pp. 1112-1126.
14. Cornwall CE, Hepburn CD, Pritchard D, Currie KI, McGraw CM, Hunter KA, Hurd CL (2012) Carbon-use strategies in macroalgae: Differential responses to lowered ph and implications for ocean acidification 1. Journal of Phycology vol. 48, no. 1, pp. 137-144.
15. De Marco P, Nóbrega CC (2018) Evaluating collinearity effects on species distribution models: An approach based on virtual species simulation. PloS one vol. 13, no. 9, pp. e0202403.
16. Department of Climate Change E, the Environment and Water (n.d.) Net Zero https://www.dcceew.gov.au/climate-change/emissions-reduction/net-zero; accessed 5 August 2025
17. Feng X, Park DS, Liang Y, Pandey R, Papeş M (2019) Collinearity in ecological niche modeling: Confusions and challenges. Ecology and evolution vol. 9, no. 18, pp. 10365-10376.

18. Flato GM (2011) Earth system models: an overview. Wiley Interdisciplinary Reviews: Climate Change vol. 2, no. 6, pp. 783-800.
19. Friedrich J, Ge M, Pickens A, Vigna L (2023) This Interactive Chart Shows Changes in the World's Top 10 Emitters https://www.wri.org/insights/interactive-chart-shows-changes-worlds-top-10-emitters; accessed 4 August 2025
20. FutureFeed (2024), FutureFeed Report to Industry 2023. Brisbane, Australia.
21. Gonzalez-Aragon D, Rivadeneira MM, Lara C, Torres FI, Vásquez JA, Broitman BR (2024) A species distribution model of the giant kelp Macrocystis pyrifera: worldwide changes and a focus on the Southeast Pacific. Ecology and Evolution vol. 14, no. 3, pp. e10901.
22. GreenerGrazing (n.d.) Farming Seaweed: Transforming Climate https://www.greenergrazing.org/; accessed 4 August 2025
23. Harisena NV, Groen TA, Toxopeus A, Naimi B (2021) When is variable importance estimation in species distribution modelling affected by spatial correlation? Ecography vol. 44, no. 5, pp.
24. Heavens NG, Ward DS, Natalie M (2013) Studying and projecting climate change with earth system models. Nature Education Knowledge vol. 4, no. 5, pp. 4.
25. Hobday AJ, Lough JM (2011) Projected climate change in Australian marine and freshwater environments. Marine and Freshwater Research vol. 62, no. 9, pp. 1000-1014.
26. Hobday AJ, Okey TA, Poloczanska ES, Kunz TJ, Richardson AJ (2006) Impacts of climate change on Australian marine life. Report to the Australian greenhouse office, Canberra, Australia vol. no., pp.
27. Kämpf J, Chapman P (2016) Upwelling systems of the world, Springer.
28. Kinley RD, Martinez-Fernandez G, Matthews MK, de Nys R, Magnusson M, Tomkins NW (2020) Mitigating the carbon footprint and improving productivity of ruminant livestock agriculture using a red seaweed. Journal of Cleaner production vol. 259, no., pp. 120836.
29. Komarek AM, Dunston S, Enahoro D, Godfray HCJ, Herrero M, Mason-D'Croz D, Rich KM, Scarborough P, Springmann M, Sulser TB (2021) Income, consumer preferences, and the future of livestock-derived food demand. Global Environmental Change vol. 70, no., pp. 102343.
30. Laeseke P, Martínez B, Mansilla A, Bischof K (2020) Future range dynamics of the red alga Capreolia implexa in native and invaded regions: contrasting predictions from species distribution models versus physiological knowledge. Biological Invasions vol. 22, no., pp. 1339-1352.
31. Li M, Zhang Y, Wallace J, Campbell E (2020) Estimating annual runoff in response to forest change: A statistical method based on random forest. Journal of Hydrology vol. 589, no., pp. 125168.
32. Ling SD (2008) Range expansion of a habitat-modifying species leads to loss of taxonomic diversity: a new and impoverished reef state. Oecologia vol. 156, no. 4, pp. 883-894.
33. Mihaila AA, Lawton RJ, Glasson CR, Magnusson M (2024) Moderate temperature and water flow increase growth during the nursery phase of Asparagopsis armata. Algal Research vol. 78, no., pp. 103380.

34. Montomoli J, Romeo L, Moccia S, Bernardini M, Migliorelli L, Berardini D, Donati A, Carsetti A, Bocci MG, Garcia PDW (2021) Machine learning using the extreme gradient boosting (XGBoost) algorithm predicts 5-day delta of SOFA score at ICU admission in COVID-19 patients. Journal of Intensive Medicine vol. 1, no. 02, pp. 110-116.
35. Myhre G, Shindell D, Bréon F-M, Collins W, Fuglestvedt J, Huang J, Koch D, Lamarque J-F, Lee D, Mendoza B (2014) Anthropogenic and natural radiative forcing. Climate Change 2013-The Physical Science Basis vol. no., pp. 659-740.
36. Nejrup LB, Pedersen MF (2012) The effect of temporal variability in salinity on the invasive red alga Gracilaria vermiculophylla. European journal of phycology vol. 47, no. 3, pp. 254-263.
37. O'Mahony J, de la Torre Cerro R, Holloway P (2021) Modelling the distribution of the red macroalgae Asparagopsis to support sustainable aquaculture development. AgriEngineering vol. 3, no. 2, pp. 251-265.
38. Oliver E, Holbrook N (2014) Extending our understanding of South Pacific gyre "spin-up": Modeling the East Australian Current in a future climate. Journal of Geophysical Research: Oceans vol. 119, no. 5, pp. 2788-2805.
39. Pereira DT, Simioni C, Filipin EP, Bouvie F, Ramlov F, Maraschin M, Bouzon ZL, Schmidt ÉC (2017) Effects of salinity on the physiology of the red macroalga, Acanthophora spicifera (Rhodophyta, Ceramiales). Acta Botanica Brasilica vol. 31, no., pp. 555-565.
40. Ridgway K, Hill K (2009) The east Australian current. vol. no., pp.
41. Rijkenberg MJ, Middag R, Laan P, Gerringa LJ, van Aken HM, Schoemann V, de Jong JT, De Baar HJ (2014) The distribution of dissolved iron in the West Atlantic Ocean. PloS one vol. 9, no. 6, pp. e101323.
42. Roleda MY, Hurd CL (2019) Seaweed nutrient physiology: application of concepts to aquaculture and bioremediation. Phycologia vol. 58, no. 5, pp. 552-562.
43. Schoffman H, Lis H, Shaked Y, Keren N (2016) Iron–nutrient interactions within phytoplankton. Frontiers in plant science vol. 7, no., pp. 196214.
44. Silva CO, Lemos MF, Gaspar R, Gonçalves C, Neto JM (2021) The effects of the invasive seaweed Asparagopsis armata on native rock pool communities: Evidences from experimental exclusion. Ecological Indicators vol. 125, no., pp. 107463.
45. Taylor S, Kumar L (2013) Potential distribution of an invasive species under climate change scenarios using CLIMEX and soil drainage: a case study of Lantana camara L. in Queensland, Australia. Journal of environmental management vol. 114, no., pp. 414-422.
46. Theobald EJ, Rule MB, Jackson TL, Rula NA, Diaz-Pulido G, Jackson EL (2024) Abiotic triggers for maximising germling numbers in Asparagopsis taxiformis (Rhodophyta, Bonnemaisoniales) via tetrasporogenesis. Journal of Applied Phycology vol. 36, no. 6, pp. 1-19.
47. Thuiller W, Georges D, Engler R, Breiner F, Georges MD, Thuiller CW (2016) Package 'biomod2'. Species distribution modeling within an ensemble forecasting framework vol. 10, no., pp. 1600-0587.2008.

48. Thuiller W, Lafourcade B, Engler R, Araújo MB (2009) BIOMOD–a platform for ensemble forecasting of species distributions. Ecography vol. 32, no. 3, pp. 369-373.
49. Tyberghein L, Verbruggen H, Pauly K, Troupin C, Mineur F, De Clerck O (2012) Bio-ORACLE: a global environmental dataset for marine species distribution modelling. Global ecology and biogeography vol. 21, no. 2, pp. 272-281.
50. UNFCCC (n.d.) The Paris Agreement https://unfccc.int/process-and-meetings/the-paris-agreement; accessed 4 August 2025
51. Varela S, Anderson RP, García-Valdés R, Fernández-González F (2014) Environmental filters reduce the effects of sampling bias and improve predictions of ecological niche models. Ecography vol. 37, no. 11, pp. 1084-1091.
52. Vergés A, Doropoulos C, Malcolm HA, Skye M, Garcia-Pizá M, Marzinelli EM, Campbell AH, Ballesteros E, Hoey AS, Vila-Concejo A (2016) Long-term empirical evidence of ocean warming leading to tropicalization of fish communities, increased herbivory, and loss of kelp. Proceedings of the National Academy of Sciences vol. 113, no. 48, pp. 13791-13796.
53. Werner A, Clarke D, Kraan S (2004), Strategic review and the feasibility of seaweed aquaculture in Ireland.
54. Wilson KL, Skinner MA, Lotze HK (2019) Projected 21st-century distribution of canopy-forming seaweeds in the Northwest Atlantic with climate change. Diversity and Distributions vol. 25, no. 4, pp. 582-602.
55. Wootton JT, Pfister CA, Forester JD (2008) Dynamic patterns and ecological impacts of declining ocean pH in a high-resolution multi-year dataset. Proceedings of the National Academy of Sciences vol. 105, no. 48, pp. 18848-18853.
56. Zanolla M, Carmona R, Mata L, De la Rosa J, Sherwood A, Barranco CN, Muñoz AR, Altamirano M (2022) Concise review of the genus Asparagopsis Montagne, 1840. Journal of Applied Phycology vol. 34, no. 1, pp. 1-17.
57. Zhu P, Li D, Yang Q, Su P, Wang H, Heimann K, Zhang W (2021) Commercial cultivation, industrial application, and potential halocarbon biosynthesis pathway of Asparagopsis sp. Algal Research vol. 56, no., pp. 102319.

# Figures

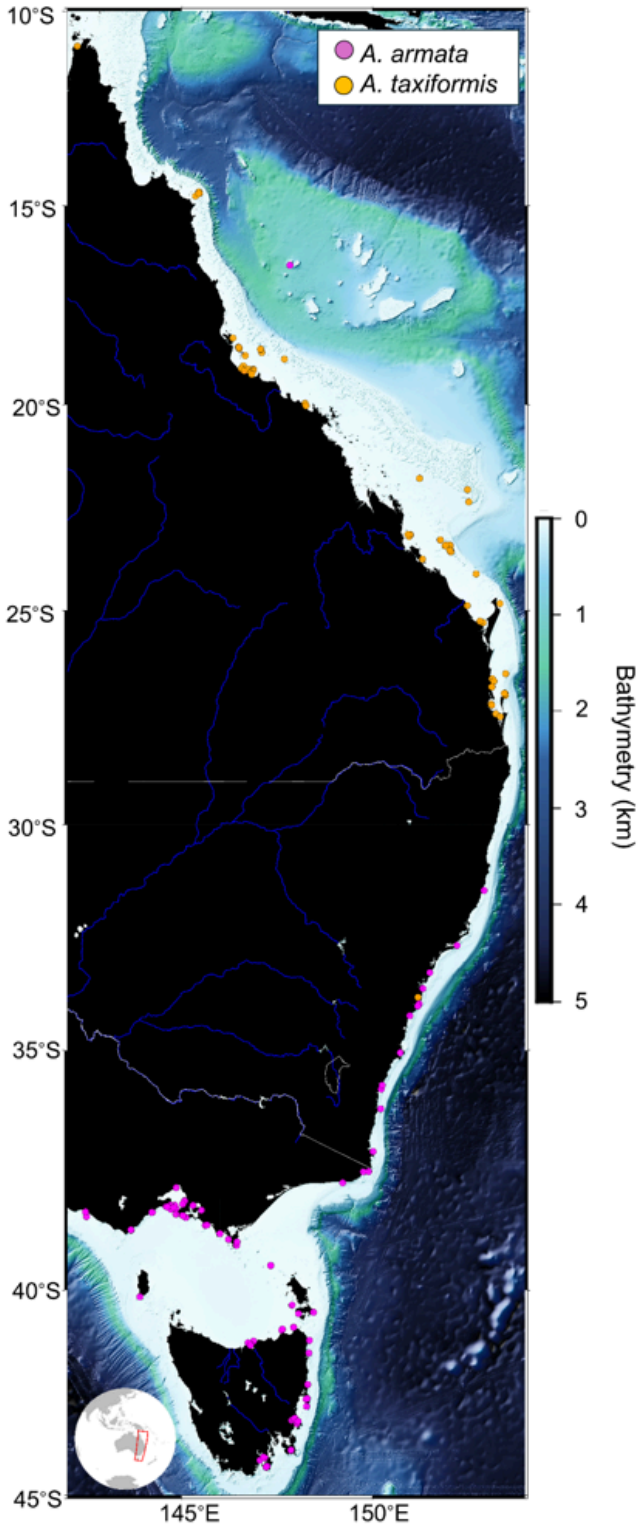


## Figure 1

The study area with *A. armata* (pink) and *A. taxiformis* (orange) occurrence points

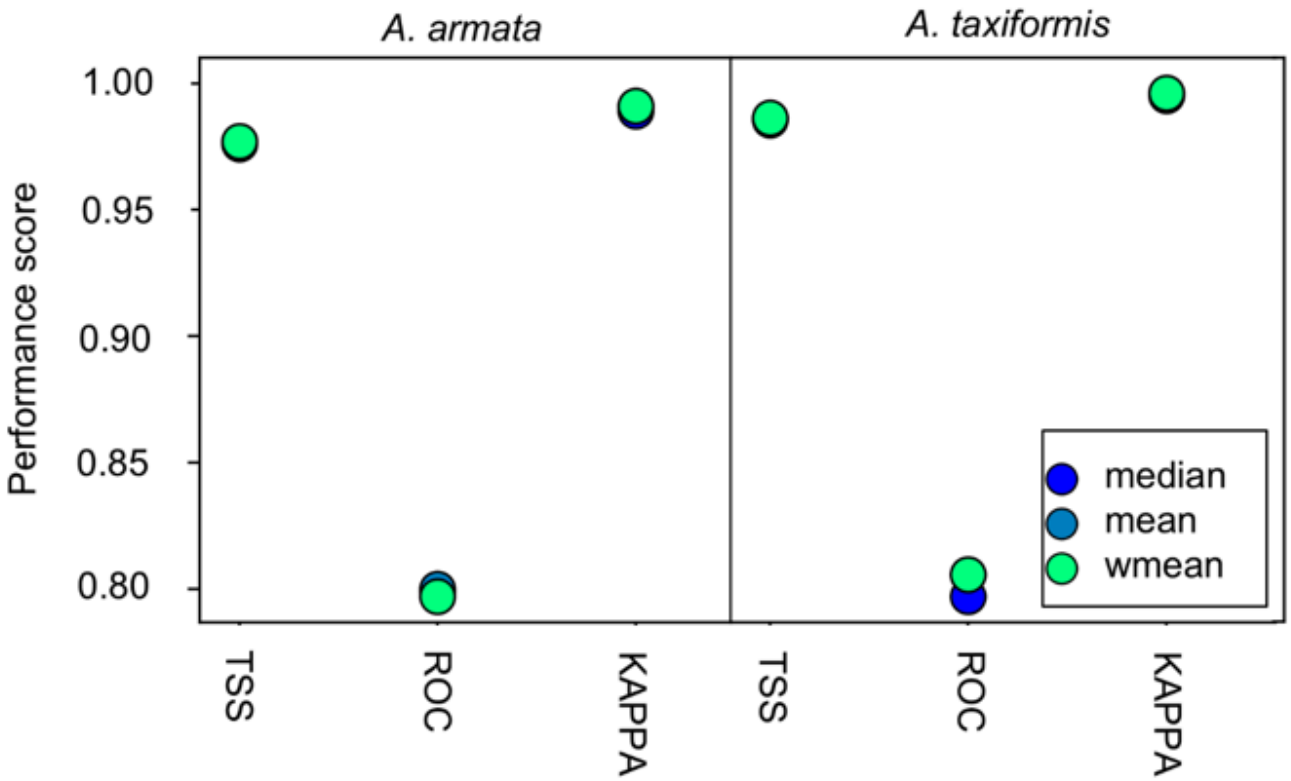


**Figure 2**

Three ensemble model performance evaluation methods with the median of probabilities, mean of probabilities and weighted mean of probabilities for *A. armata* and *A. taxiformis*

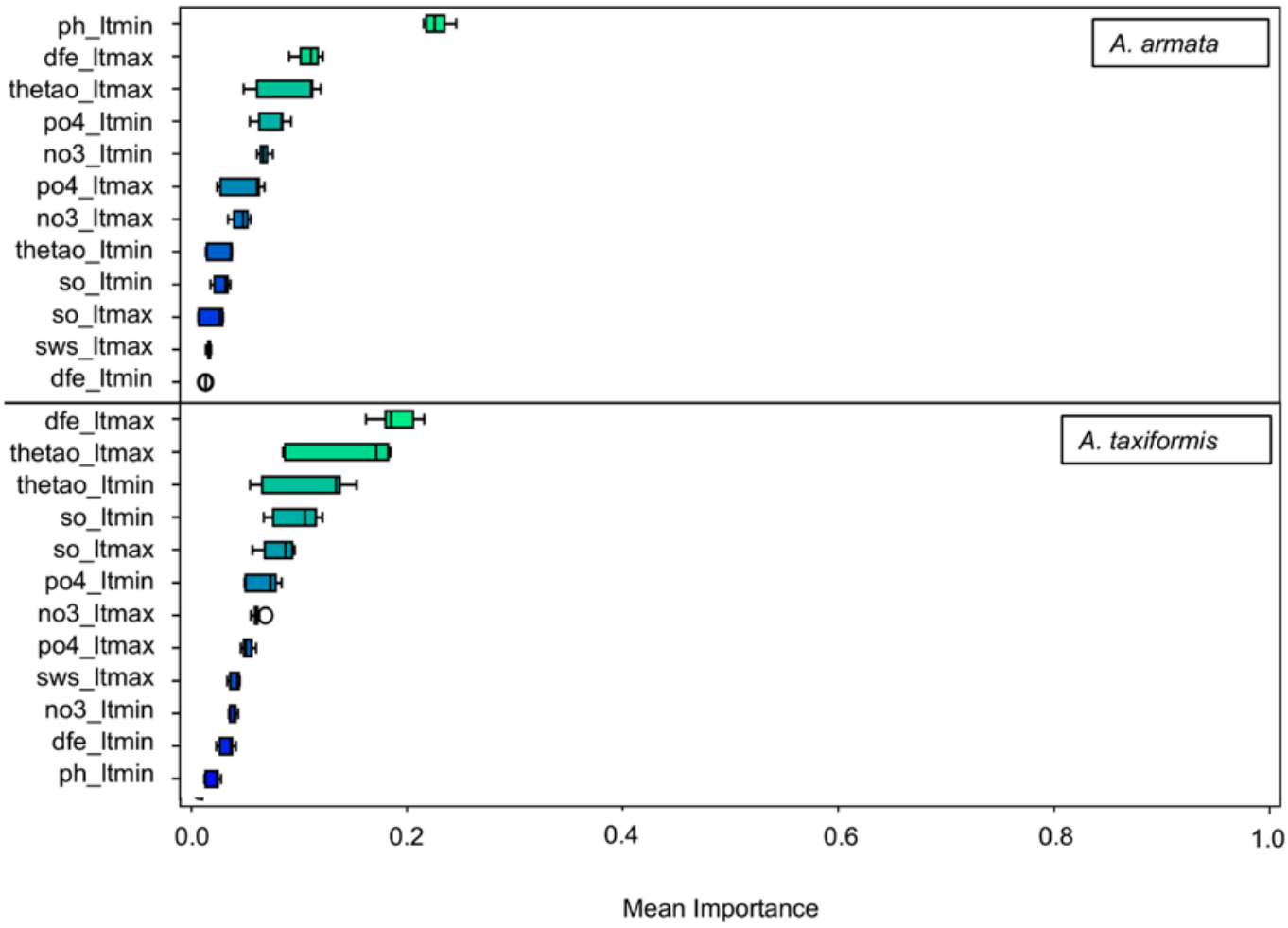


## Figure 3

Box plot representing the 25$^{th}$ to 75$^{th}$ Interquartile Range (IQR) of the relative importance of the environmental factors that contribute to the habitat distribution in the ensemble model for A. armata and A. taxiformis in 2010. Whiskers represent 1.5 times IQR, black lines represent median, and circle represent outliers.

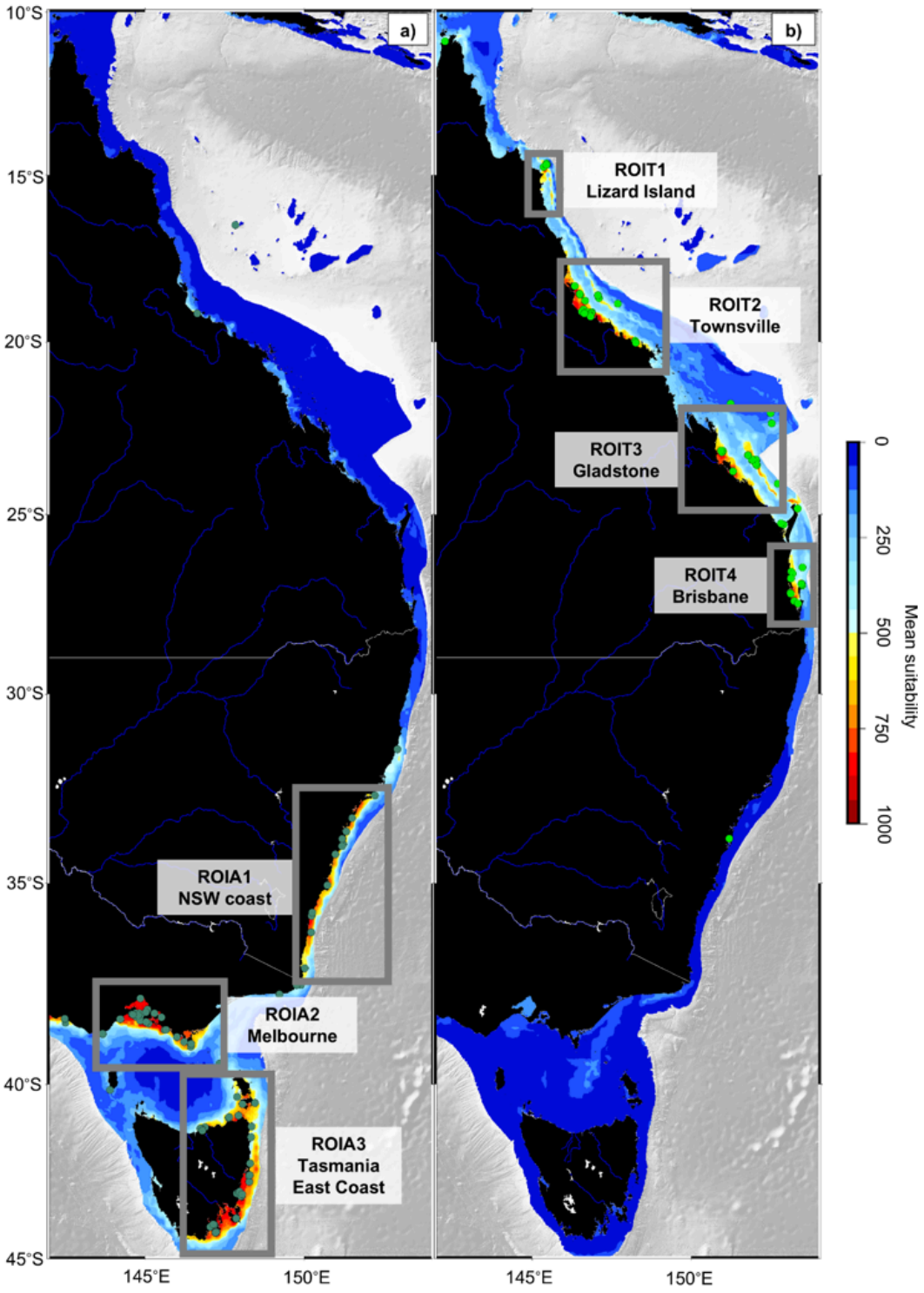


## Figure 4

Projection of mean habitat suitability (0 – 1000) for *A. armata* **(a)** and *A. taxiformis* **(b)** on Australia's East Coast with overlayed occurrence data of the respective species.

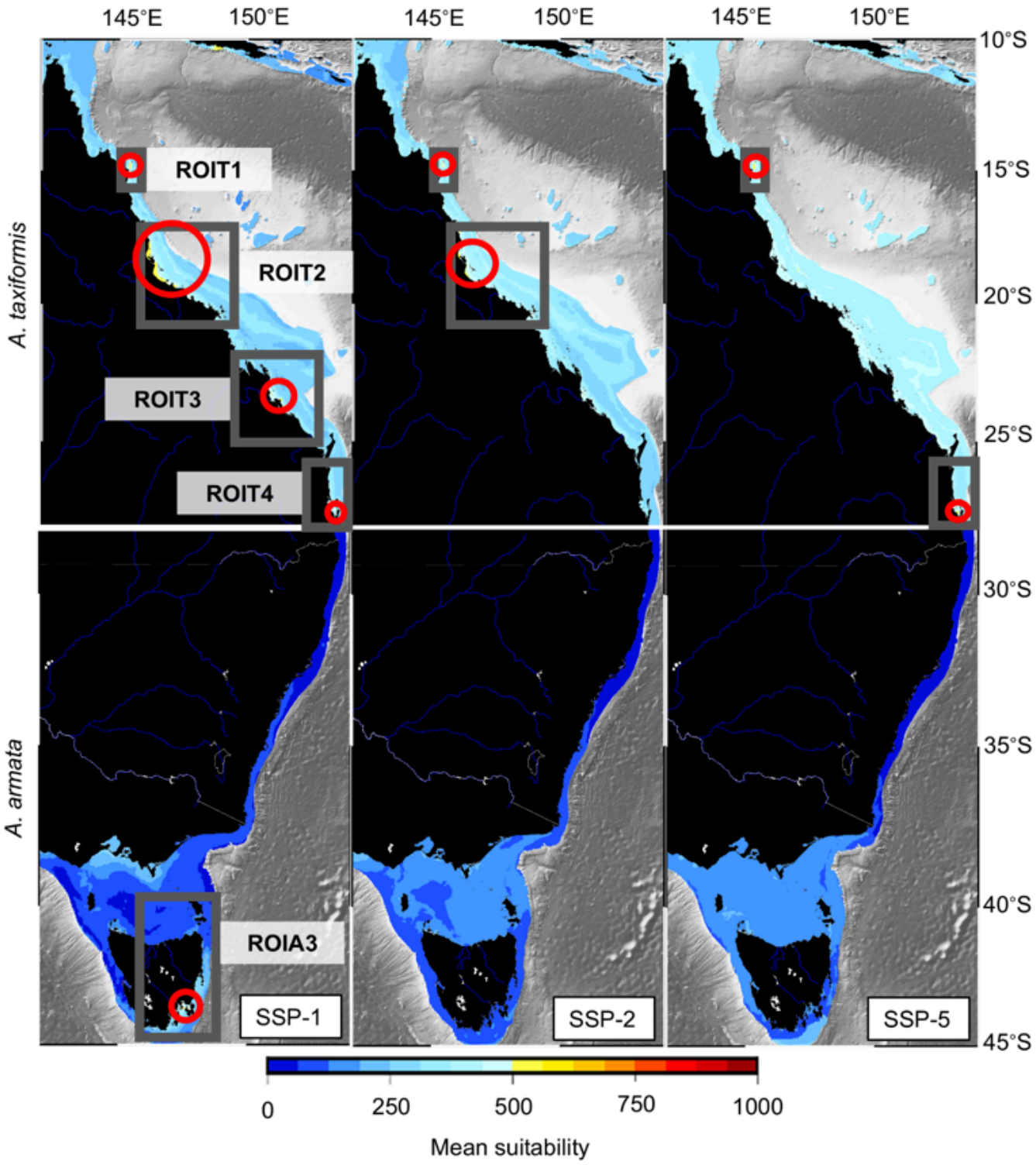


## Figure 5

Projections of mean habitat suitability (0 - 1000) of *A. taxiformis* (top) and *A. armata* (bottom) in 2100 under SSP-1, SSP-2, and SSP-5. Regions of interest (ROI) have been boxed and named with an A for *A. armata* or T for *A. taxiformis* and numbered from north to south. Red circles highlight areas of moderate suitability within ROIs.

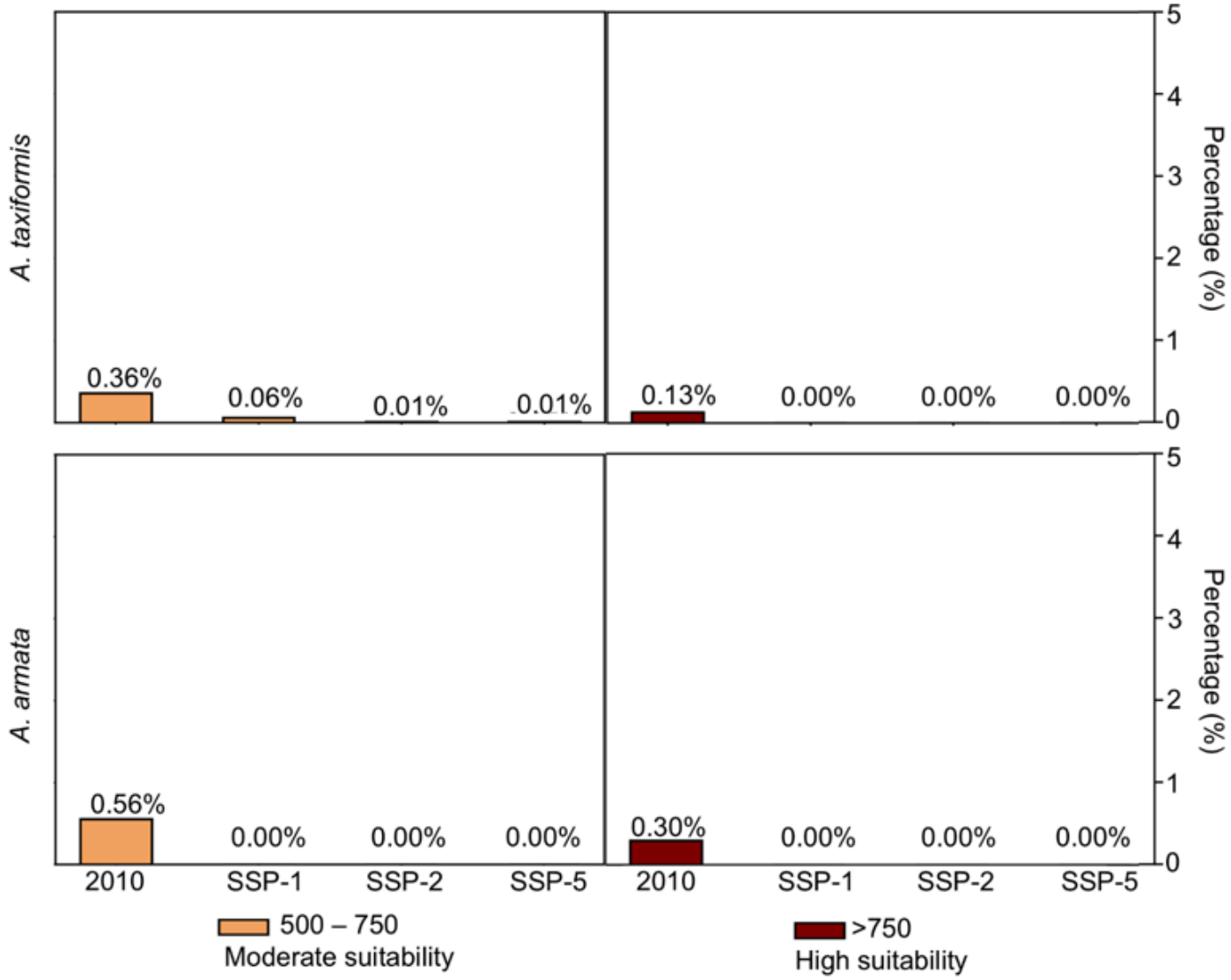


## Figure 6

Bar graphs of the percentage of study area which is highly (750 – 1000) and moderately (500 – 250) suitable in 2010 and 2100 under SSP-1, SSP-2 and SSP-5 for *A. taxiformis* (top) and *A. armata* (bottom)